OBSERVATIONAL EVIDENCE OF IMPACTS OF AEROSOLS ON SEASONAL-TO-INTERANNUAL VARIABILITY OF THE ASIAN MONSOON

K.-M. Lau, K.-M. Kim, and N. C. Hsu
Laboratory for Atmospheres, NASA/Goddard Space Flight Center

Popular Summary

There is a growing body of scientific evidence suggesting that aerosol may affect clouds, rainfall and the water cycle. In Asian monsoon regions, which occupies over 60% of the world population, aerosol is an increasing acute problem because of industrialization, transport of dust from dust storms in adjacent deserts, and biomass burning from agricultural practices and forest fires. On the other hand, flood or drought associated with extreme fluctuation of the monsoon water cycle is the number-one natural disaster afflicting human societies and diverse eco-systems in these regions. Recent studies from computer model simulations have suggested that increasing aerosol loading in the tropical atmosphere, particularly over the Indo-Gangetic Plain and over the southern slopes of the Tibetan Plateau may have strong impacts on the variability of rainfall in the South Asia monsoon. Validation of these model results is crucial to advancing our understanding of aerosol-water cycle interaction, monsoon weather and climate change and impacts on human society.

In this paper, we use long-term (more than 2 decades) atmospheric aerosol concentration estimated from the NASA Total Ozone Mapping Spectrometer (TOMS), and ancillary data to show that the Indian subcontinent and surrounding regions are subject to heavy loading of a special type of aerosols that absorb solar radiation (dust and black carbon), and therefore heat the atmosphere. These aerosols have strong seasonality closely linked to the monsoon annual rainfall cycle. Increased loading of absorbing aerosols over the Indo-Gangetic Plain in April-May is associated with a) increased heating of the upper troposphere over the Tibetan Plateau, b) an advance of the monsoon rainy season, and c) subsequent enhancement of monsoon rainfall over the South Asia subcontinent, and reduction over East Asia. Also presented are radiative transfer calculations showing how differential solar absorption by aerosols over bright surface (desert or snow cover land) compared to dark surface (vegetated land and ocean), may be instrumental in triggering an aerosol-monsoon large-scale circulation and water cycle feedback, providing observational support of the so-called "elevated heat pump" hypothesis (*Lau et al.* 2006).

OBSERVATIONAL EVIDENCE OF IMPACTS OF AEROSOLS ON SEASONAL-TO-INTERANNUAL VARIABILITY OF THE ASIAN MONSOON

K.-M. Lau, K.-M. Kim, and N. C. Hsu

Laboratory for Atmospheres, NASA/Goddard Space Flight Center

February 2006

(Submitted to Geophys. Res. Letters)

Corresponding author: K. M. Lau, Laboratory for Atmospheres, NASA Goddard Space Flight Center, Greenbelt, MD. Email:.william.k.lau@nasa.gov, Tel: 301-614-6332

Abstract

Observational evidences are presented showing that the Indian subcontinent and surrounding regions are subject to heavy loading of absorbing aerosols (dust and black carbon), with strong seasonality closely linked to the monsoon annual rainfall cycle. Increased loading of absorbing aerosols over the Indo-Gangetic Plain in April-May is associated with a) increased heating of the upper troposphere over the Tibetan Plateau, b) an advance of the monsoon rainy season, and c) subsequent enhancement of monsoon rainfall over the South Asia subcontinent, and reduction over East Asia. Also presented are radiative transfer calculations showing how differential solar absorption by aerosols over bright surface (desert or snow cover land) compared to dark surface (vegetated land and ocean), may be instrumental in triggering an aerosol-monsoon large-scale circulation and water cycle feedback, consistent with the "elevated heat pump" hypothesis (*Lau et al.* 2006)

1. Introduction

Absorbing aerosols such as dust and black carbon are characterized by its ability to heat the atmosphere by absorbing solar radiation. In contrast, non-absorbing aerosols such as sulfate, scatters solar radiation and have relatively weak atmospheric heating effect. Yet, both absorbing and non-absorbing aerosols cause surface cooling by blocking solar radiation from reaching the earth surface – the so-called "global dimming" effect [*Stanhill and Cohen,* 2001]. In Asian monsoon regions, the dimming effect is especially large due to heavy pollution, and frequent occurrence of dust storms [*Kaiser and Qian 2002*, *Singh et al.* 2004]. From coupled general circulation model (GCM) experiments, *Ramanathan et al.* [2005] showed that global dimming causes a long-term (multi-decadal) weakening of the South Asian monsoon by reducing the meridional surface temperature gradient between the Asian land mass and the Indian Ocean. However dimming is not the only mechanism that may affect the Asian monsoon water cycle. , *Menon et al.* [2002] showed that atmospheric heating induced by increasing loading of black carbon in the Asian monsoon region may be responsible for the long-term dry (wet) pattern over northern (southern) China. *Lau et al.* [2006] demonstrated, that heating by absorbing aerosols (dust and black carbon) may accelerate the seasonal heating of the upper troposphere over the northern India and southern slopes of the Tibetan regions in late spring and early summer, subsequently leading to an intensification of the Indian monsoon. While these studies indicate plausible but different scenarios of aerosol impacts, they suggest that aerosol effects on monsoon water cycle dynamics are extremely complex, and strongly dependent on aerosol distribution and characteristics, as well as on spatial and temporal scales.

In this article, we present observational evidences that generally support the so-called "Elevated Heat Pump" (EHP) effect [*Lau et al*, 2006], i.e., solar absorption by dust transported from the deserts in Pakistan/Afghanistan, the Middle East, and the Sahara, and driven up against the southern slopes of the Himalayas in late spring and early summer, provides an efficient large

scale elevated heat source that accelerates the seasonal heating over the Tibetan Plateau. The dust combined with the black carbon from industrial and agricultural pollution in northern India provide an anomalous diabatic heat source, which interacts with in monsoon convective heating, leading to increased rainfall over northern India and the Bay of Bengal. For aerosol observation, we use the Total Ozone Mapping Spectrometer (TOMS) Aerosol Index (AI). The AI data set is the only long-term continuous daily global record for absorbing aerosols, starting in November 1978 and, with the exception of a data gap from May 1993 to August 1996, to the present. For rainfall, we use the Global Precipitation Climatology Precipitation (GPCP) data [*Huffman et al., 1997*], which combines surface rain gauge data as well as merged satellite estimates covering the period 1979-present.

2. Results

a. Variability of absorbing aerosols and relationship with monsoon rainfall

Figure 1a shows the April-May climatological (1979-1992) distribution of AI absorbing aerosols over the greater Indian monsoon region. Three major source regions can be identified: (I) The Indo-Gangetic Plain over northern India, including the Thar Desert (marked by the rectangular box in Fig. 1b), (II) Saudi Arabia and Iran/Afghanistan/Pakistan deserts, and (III) Western Asia over the Taklamakan desert. The interannual variability of the aerosol loading (Fig. 1b) is found to be about 10-15% of the bimonthly mean, and is strongest over the Middle East (Region II), but significant over Region I and III. Aerosol radiative forcing from these regions may alter the large-scale thermal contrast in the troposphere and between the land surface and the adjacent oceans. In addition, dusts from Regions II may be transported to Region I, through low level monsoon westerlies and mix with the black carbon produced from local emissions, further altering the atmospheric heat source and sink distribution. Since aerosol emission, concentration and transport is dependent on the large scale circulation and the rainfall, the total dust loading in all three source regions undergo multi-scale variability associated with the monsoon climate system. Observations by the Aerosol Robotic Observation Network (AERONET) in Kanpur

over northern Indian has confirmed that much of the aerosols in Region I consist of coarse particles, characteristic of dust [*Singh et al* 2004]. The estimated single scattering albedo (approximately 0.90 – 0.92) suggests that they are moderate to strong absorber of solar radiation, mostly composed of dust particles coated with anthropogenic black carbon.

Fig. 1c shows the AI in Region I, superimposed on the monthly all-India rainfall for years 1987-1991. Most conspicuous is the strong seasonality of the aerosol loading, rising rapidly in boreal spring (March-April-May), peaking near the latter part of May, just before the start of the monsoon rainy season over India, and declining during the summer monsoon and the following seasons. The intraseasonal and interannual variability of aerosol amount are also strong. Since excessive monsoon rainfall is expected to wash out more aerosols, the AI variability may also indicate strength of the monsoon. For example, in 1988, removal of aerosol from the atmosphere is very rapid, with the aerosol reaching minimum levels soon after the excessive rain over all India in June. In contrast, in 1987, the removal of aerosols is relatively slow, consistent with a delayed and weakened monsoon. Previous studies have reported that by all measures, 1988 (1987) was a strong (weak) monsoon year [*Ji and Vernekar*, 1997; and many others]. This is also obvious from the all-India rainfall shown in Fig. 1c. Yet all previous studies of the 1987-88 Indian monsoon were almost exclusively focused on the effects of SST forcing, and without conclusive results. We note from Fig.1c that the build-up of absorbing aerosol is abnormally strong in the spring season leading up to the monsoon season in 1988, and mush less so in 1987. Similarly, in 1991, the all-India rainfall in May increased following a spike in the AI in early May and rain increased further in June following a second spike of AI in late May or early June. These observations are obviously anecdotal, but they do beg the question, whether a strong build up of aerosol in spring can be a contributing factor to an intensification of the monsoon.

To show that aerosol may be a causal factor in monsoon rainfall anomalies, composite latitude-time cross sections of AI and rainfall over Region I for four years (1980, 1985, 1988,1991) of anomalously high AI (> one standard deviation) have been computed. Fig. 2a

shows a slow build up of the aerosol beginning early spring leading to a maximum in mid-May, followed by a rapid removal in June-July-August. There appears to be a northward migration of rainfall anomaly from equatorial oceanic region to the monsoon land region, and an intensification of the monsoon rainfall (15–20° N) in June-July (Fig.2b), presaged by the aerosol build-up in May. Over the Indian subcontinent, and the Indian ocean to the south (0-30° N), the rainfall season seems to have advanced with more rain appears in the early part, and less rain in the latter part of the season. Fig. 2c shows that the rainfall increase in June-July is over the entire Indian subcontinent, with most pronounced signal over the Western Ghats, and the land region around the Bay of Bengal. The strengthened Indian monsoon is also evident in the anomalous low level westerlies over the Indian subcontinent. Over East Asia, a strong anticyclonic anomaly is found, suggesting an intensification and a westward shift of the Western Pacific Subtropical High. As a result, rainfall over South China is reduced, with the *Mei-yu* rainbelt pushed north of the Yangtze and eastward over Japan, reminiscent of the well-known north-south dipole rainfall anomaly over East Asia [*Lau et al.*, 2000].

b. Aerosol radiative forcing

The aforementioned discussions suggest that a large-scale dynamical modal response in the entire Asian monsoon system may have been triggered by aerosol forcing. But, how can absorbing aerosols over Asia continent trigger such a large-scale dynamical monsoon response? . We also recalled that the net radiative effect of aerosols on the atmosphere and the surface depends not only on the aerosol type but also on the albedo and the temperature of the underlying surface [Hsu *et al.*, 2000]. To illustrate this, we have computed the shortwave radiative forcing, due to a dust layer of unit optical thickness over a bright land surface with albedo = 0.35, and over dark ocean surface with albedo = 0.03 respectively. The longwave forcing from dust is generally small compared to the shortwave forcing and is not as well quantified due to the uncertainty in the dust properties in the infrared regime. [*Haywood et al.*, 2005]. The spectral dust properties used in the calculations are based upon values reported in Optical Properties of

Aerosols and Clouds (OPAC) for 0.5 μm dust particles [*Hess et al.*, 1998], in which the corresponding equivalent broadband single scattering albedo is approximately 0.92, consistent with the AERONET observation over Kanpur in northern India [*Singh et al* 2004, *Dey et al* 2004]. The calculations are conducted using a climatological atmospheric temperature and moisture sounding over land, and over ocean respectively. The aerosol forcing is defined as the difference in radiation flux between the same atmospheres, with and without aerosols (see Table 1). Over both ocean and land, the dust aerosol cools the earth surface due to the "dimming" effect. However, the land surface is cooled less (-107 Wm^{-2}) compared to the ocean. (-175 Wm^{-2}). The differential cooling stems from multiple reflections of solar radiation between the high-albedo land surface and the dust layer, leading to enhanced absorption by the dust layer, as evidenced in the less reduction of incoming solar radiation, and diminished reflected solar radiation over land. As a result, there is a *net loss* of solar radiation at the-top-of-the-atmosphere (TOA) for the atmosphere-ocean system, (-78 Wm^{-2}), in contrast to a *net gain* at the TOA of atmosphere-land system (8 Wm^{-2}). The net result is that the atmosphere over ocean is heated by 97 Wm^{-2}, (computed as the surface minus the top-of-the atmosphere fluxes) while over land the heating by the same aerosol is significantly stronger at 115 Wm^{-2}. As demonstrated in the EHP effect [*Lau et al. 2006*], when the aerosol layer is close to the elevated high-albedo surface such as the Himalayas, the atmospheric heating by aerosols, coupled with the turbulent heat exchange between the atmosphere and the elevated land surface may actually reverse the sign of the net aerosol forcing at the surface and cause the land surface to warm. Such warming may amplify the seasonal heating of the Tibetan Plateau by sensible heat flux in late spring, causing an early reversal of the meridional temperature gradient in the upper troposphere between the land region and the oceanic region to the south, and subsequently leading to an advance of the monsoon season, and intensification of monsoon.

c. Upper tropospheric temperature anomalies

The importance of the north-south tropospheric temperature gradient in late spring in affecting the subsequent evolution of the entire Asian monsoon has been documented in many previous studies [*Yanai et al.*, 1992; *Li and Yanai*, 1996; *He et al.*, 2003, and many others]. Recently *Goswami and Xavier* [2005] used long-term daily data to construct a monsoon index (ΔTT in their paper) based on the difference in the averaged temperature in the layer 700-200 hPa between the northern India/Tibetan Plateau [10°N-35°N, 30°E-110°E] to the mostly oceanic region [15°S-10°N, 30°E-110°E] to the south, and showed that the reversal in sign of this index is highly correlated to the onset and withdrawal of the rainfall over India. To further examine the relationship between monsoon variability and AI, we have constructed the ΔTT monsoon index based on daily temperature from NCEP (1979-2000), and computed the correlations with de-trended AI. From the one-point correlation map of ΔTT with AI (Fig. 3a), it can be seen that when ΔTT is positive (anomalous high tropospheric temperature over Tibetan Plateau relative to oceanic region to the south), the Indian subcontinent and the surrounding region all show above-normal high concentration of absorbing aerosols, while the regions south of 10° N show below-normal concentration. Conversely, when the AI over Region I is correlated with the upper tropospheric temperature anomalies in April-May, we find a clear signal of above-normal temperature over the northern Indian, Tibet and East Asia, and below-normal temperature in regions south of 10° N. (Fig. 3b). A temperature anomaly such as shown in Fig. 3b, will facilitate an early onset of the South Asian monsoon, as demonstrated by *Goswami and Xavier* [2005]. In this case, the temperature anomaly is associated with the increased concentration of aerosol over the northern India. The relationship between upper tropospheric temperature and AI support our calculations of aerosol induced radiative heating in Section 2b.

3. Concluding remarks

Our observation results and calculations are consistent with the EHP mechanism by which absorbing aerosol may lead to enhanced monsoon rain over India on seasonal-to-interannual timescales [*Lau et al.*, 2006]. The long-term effect of the mechanism is not yet known, but is

being investigated. We stress that, because of the limited samples used, the results of this work should not be judged entirely on statistics, but rather on physical basis underlying the relationships, and consistency with the EHP mechanism for aerosol-monsoon dynamical interactions. These results will provide guidance and new avenues for exploring monsoon variability and predictability. Based on results of this and other contemporary studies, it is argued that aerosol forcing on monsoon water cycle is a factor we can no longer afford to ignore, and should be examined in conjunction with SST, land surface forcing and other agents of change for monsoon climate variability and change.

Acknowledgment

This work is partially supported by the TRMM project, and the Modeling and Analysis Program, NASA Earth-Sun Division, Science Mission Directorate.

Reference

Dey, S., S. N. Tripathi and R. P. Singh (2004), Influence of dust storms on the aerosol properties over the Indo-Gangetic basin. *J. Geophys. Res.*, **109**, D20211, doi:10.1029/2004JD004924

He, H., C. –H. Sui, M. Jian, Z, Wen, and G, Lan (2003), The evolution of upper tropospheric temperature field and its relationship with the onset of the Asian summer monsoon, *J. Meteor. Soc. Japan, 81*, 1201-1223.

Goswami, B. N. and P.K. Xavier (2005), ENSO control on the South Asian monsoon through the length of rainy season. *Geophys. Res. Lett. 32 (18)*, Art. No. L18717.

Haywood, J. M., R. P. Allan, I. Culverwell, T. Slingo, S. Milton, J. Edwards, and N. Clerbaux (2005), Can desert dust explain the outgoing longwave radiation anomaly over the Sahara during July 2003?, *J. Geophys. Res.*, 110, D05105, doi:10.1029/2004JD005232.

Hess, M, P. Koepke, and I. Schult (1998), Optical Properties of Aerosols and clouds: The software package OPAC, *Bull. Am. Met. Soc., 79*, 831-844.

Hsu, N.C., J. R. Herman, , J. F. Gleason, , O. Torres, , and C. J. Seftor, (1999), Satellite detection of smoke aerosols over a snow/ice surface by TOMS, *Geophys. Res. Lett., 26*, 1165-1168.

Hsu, N. C., J. R. Herman, and C. Weaver (2000), Determination of radiative forcing of Saharan dust using combined TOMS and ERBE data, *J. Geophys. Res.*, 105, 20,649 - 20,661.

Huffman, G., R. Adler, P. Arkin, A. Chang, R. Ferraro, A. Gruber, J. Janowiak, A. McNab, R. Rudolf and U. Schneider (1997), The Global Precipitation Climatology Project (GPCP) combined precipitation dataset. *Bull. Am. Metor. Soc., 78*, 5-20.

Ji, Y., and A. D. Vernekar (1997), Simulation of the Asian Summer Monsoons of 1987 and 1988 with a regional model nested in a global GCM, J. Climate, 10, 1965-1979.

Kaiser, D. P., and Y. Qian (2002), Decreasing trends in sunshine duration over China for 1954-1998: Indication of increased haze pollution? Geophys. Res. Lett., 29, 2042, doi:10.1029/2002GL016057.

Lau, K. M., K. M. Kim, and S. Yang (2000), Dynamical and Boundary Forcing Characteristics of regional components of the Asian summer monsoon, *J. Climate, 13,* 2461-2482.

Lau, K. M., M. K. Kim and K. M. Kim (2006), Asian monsoon anomalies induced by aerosol direct effects – the role of the Tibetan Plateau *Climate Dynamics*, doi:10.1007/s00382-006-0114-z..

Li, C., and M. Yanai (1996), The onset and interannual variability of the Asian summer monsoon in relation to land-sea thermal contrast, *J. Climate,* 9, 358-375.

Menon, S., J. Hansen, L. Nazarenko, and Y. Luo (2002), Climate effects of black carbon aerosols in China and India. *Science, 297*, 2250-2253.

Ramanathan V., C. Chung, D. Kim, T. Betge, L. Buja, J. T. Kiehl, W. M. Washington, Q. Fu, D. R. Sikka, and M. Wild (2005), Atmospheric brown clouds: impacts on South Asian climate and hydrological cycle, *Proc. Natl. Acad. Sci., 102*, 5326-5333, doi: 10.1073/pnas.0500656102.

Singh, R. P., S. Dey, S. N. Tripathi, and T. Vinde, B. Holben (1994): Variability of aerosols parameters over Kanpur, northern India. *Geophys. Rev. Lett,* **109**, D23206, doi:10.1029/2004JD004966.

Stanhill, G., and S. Cohen (2001), Global dimming, a review of the evidence for a widespread and significant reduction in global radiation with a discussion of its probable causes and possible agricultural consequences, *Agric. For. Meteorol., 107*, 255-278.

Yanai, M., C. F. Li, and Z. S. Song (1992), Seasonal heating of the Tibetan Plateau and its effects on the evolution of the Asian summer monsoon, *J. Meteor. Soc. Japan, 70*, 319-351.

Figure Captions

Figure 1 Climatological (1979- 2001) distribution of absorbing aerosols over the Indian subcontinent and adjacent areas based on the TOMS Aerosol Index (AI) for April-May showing a) the bi-monthly mean distribution, and b) the monthly standard deviation, and c) Area mean daily AI, and total rainfall (bar charts) over Region I. Key source regions are marked by numbered rectangles in b). Shaded columns mark the March-April-May season. AI is in normalized unit, and rainfall unit is in $mmday^{-1}$.

Figure 2 Time-latitude cross-sections showing composite seasonal evolution during year of high loading of absorbing aerosols of a) the AI anomalies, and b) the observed rainfall anomalies, and c) composite of rainfall and 850 hPa wind pattern during years of high AI anomalies. Unit of rainfall is in $mmday^{-1}$, and wind is $msec^{-1}$.

Figure 3 One-point correlation map showing spatial distribution of a) AI with the ΔTT monsoon index, and b) mean tropospheric (700-200 hPa) temperature with AI over northern India. Regions exceeding 95% confidence level are shaded.

Table 1a Anomalous downward ($\downarrow\Delta_{sw}$) and upward ($\uparrow\Delta_{sw}$) solar radiation, and aerosol radiative forcing (ARF) at the top of the atmosphere (TOA), surface (SFC) and the atmosphere (ATM) for a layer of dust with unit aerosol optical thickness, for a standard atmosphere over a dark ocean with albedo =0.03. Positive ARF indicates heating effect. Unit is in Wm^{-2}.

	$\downarrow\Delta_{sw}$	$\uparrow\Delta_{sw}$	ARF= $\downarrow\Delta_{sw}$ - $\uparrow\Delta_{sw}$
TOA	0	78	-78
SFC	-180	- 5	-175
ATM (TOA – SFC)	180	83	97

Table 1b. Same as Table 1a, except over desert land surface with albedo =0.35

	$\downarrow\Delta_{sw}$	$\uparrow\Delta_{sw}$	ARF= $\downarrow\Delta_{sw}$ - $\uparrow\Delta_{sw}$
TOA	0	-8	8
SFC	-144	- 37	-107
ATM (TOA – SFC)	144	29	115

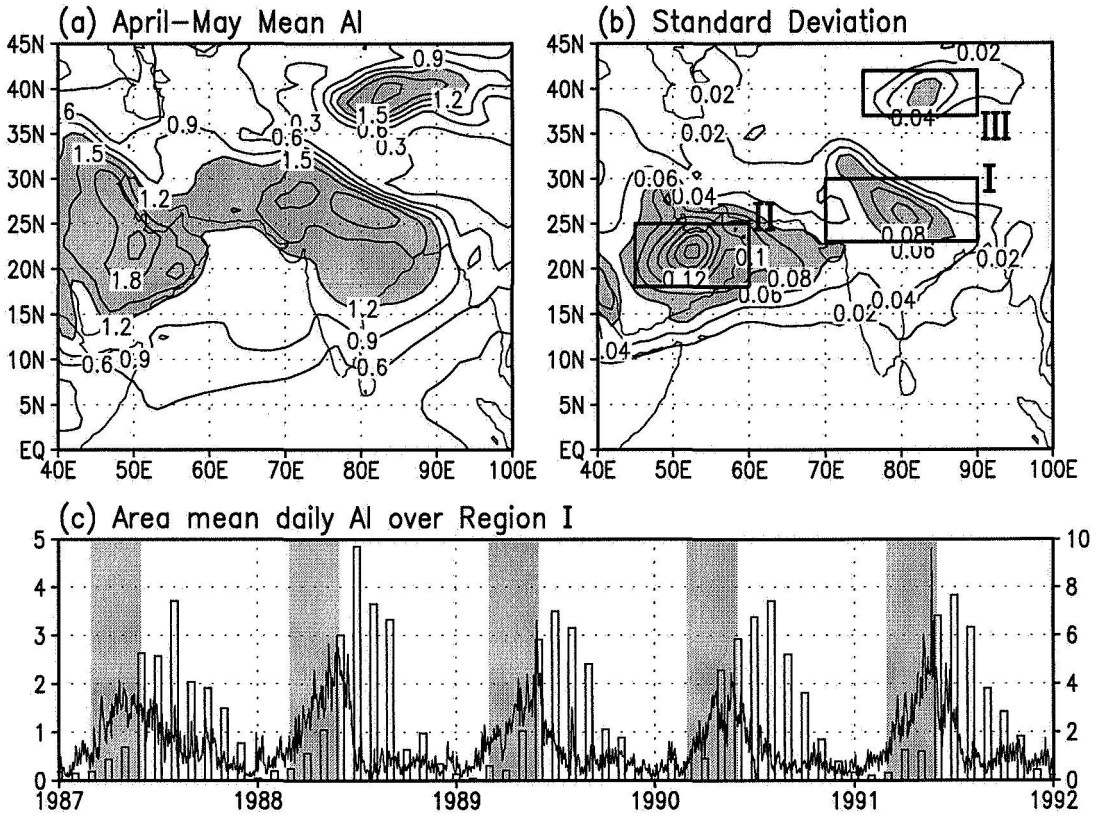
(a) April–May Mean AI
(b) Standard Deviation
(c) Area mean daily AI over Region I
I
II
III
45N
40N
35N
30N
25N
20N
15N
10N
5N
EQ
40E
50E
60E
70E
80E
90E
100E
1987
1988
1989
1990
1991
1992

Figure 1

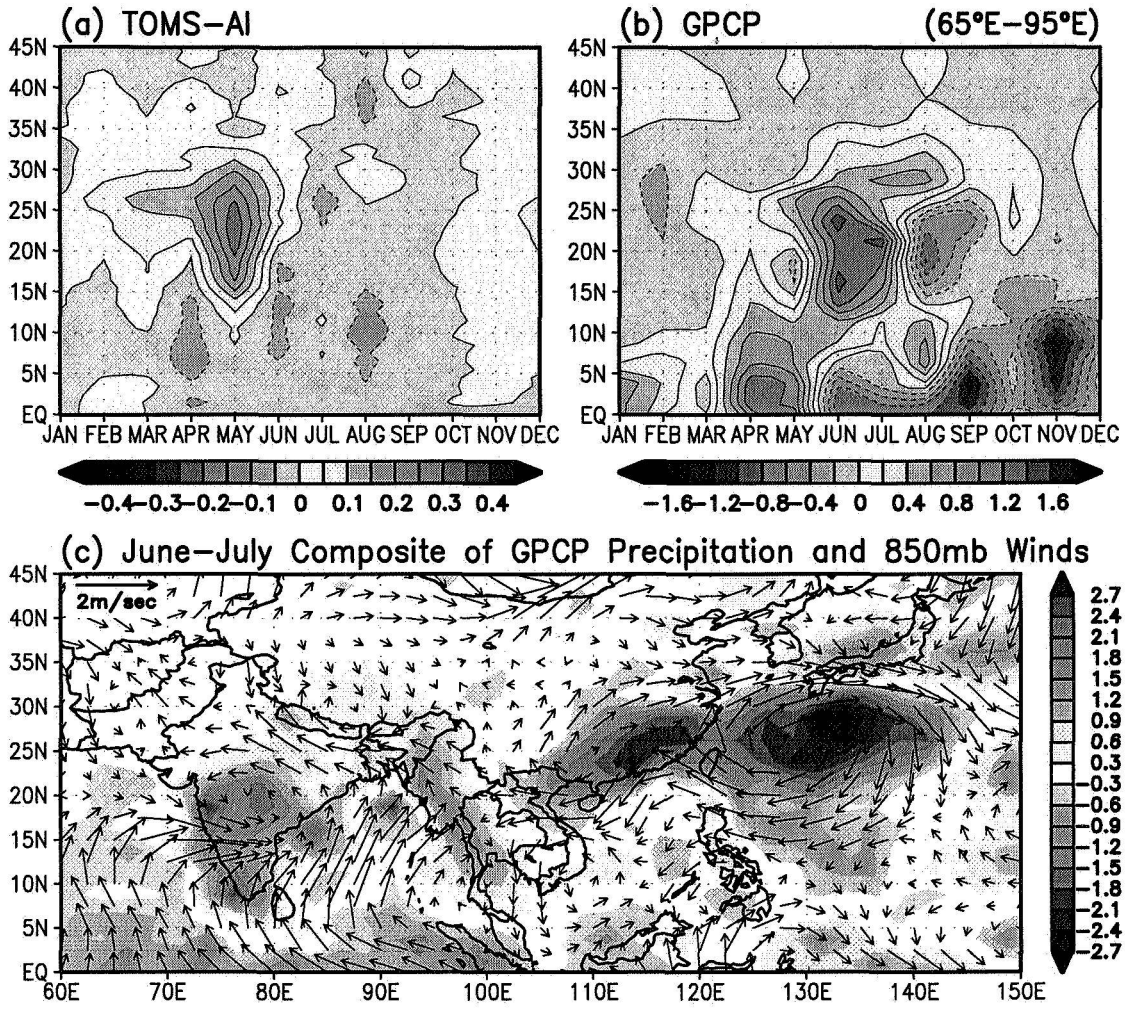
(a) TOMS-AI
(b) GPCP
(65°E-95°E)
45N
40N
35N
30N
25N
20N
15N
10N
5N
EQ
JAN FEB MAR APR MAY JUN JUL AUG SEP OCT NOV DEC
-0.4 -0.3 -0.2 -0.1 0 0.1 0.2 0.3 0.4
-1.6 -1.2 -0.8 -0.4 0 0.4 0.8 1.2 1.6
(c) June-July Composite of GPCP Precipitation and 850mb Winds
2m/sec
60E
70E
80E
90E
100E
110E
120E
130E
140E
150E
2.7
2.4
2.1
1.8
1.5
1.2
0.9
0.6
0.3
-0.3
-0.6
-0.9
-1.2
-1.5
-1.8
-2.1
-2.4
-2.7

Figure 2

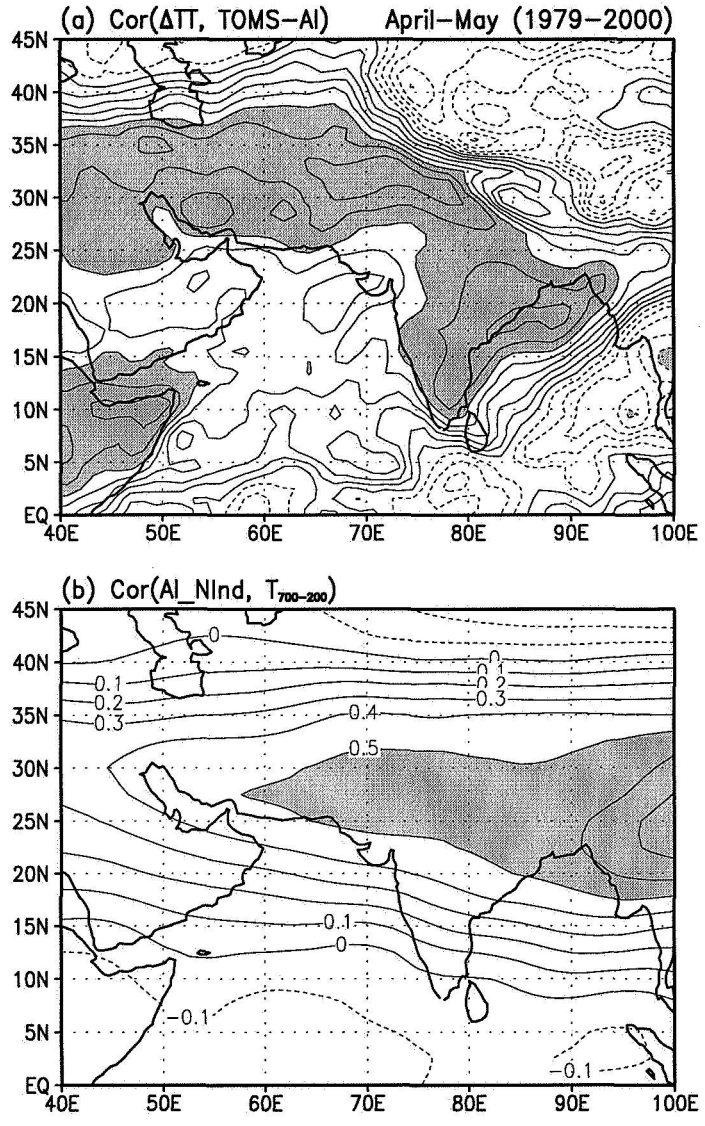
(a) Cor(ΔTT, TOMS−AI) April−May (1979−2000)
45N
40N
35N
30N
25N
20N
15N
10N
5N
EQ
40E
50E
60E
70E
80E
90E
100E
(b) Cor(AI_NInd, T700−200)
0
0.1
0.2
0.3
0.4
0.5
−0.1

Figure 3